A Journal of the Gesellschaft Deutscher Chemiker

Angewandte International Edition GDCh Chemie

www.angewandte.org

Accepted Article

Title: Ultralow lattice thermal conductivity at room temperature in Cu4TiSe4

Authors: Biplab Koley, Achintya Lakshan, Parul R. Raghuvanshi, Charanpreet Singh, Amrita Bhattacharya, and Partha Pratim Jana

To be cited as: *Angew. Chem. Int. Ed.* 10.1002/anie.202014222

Link to VoR: https://doi.org/10.1002/anie.202014222

WILEY-VCH

10.1002/anie.202014222

Ultralow lattice thermal conductivity at room temperature in Cu_4TiSe_4

Biplab Koley[†], Achintya Lakshan[†§], Parul R. Raghuvanshi,[†† §]Charanpreet Singh[#§], Amrita Bhattacharya*[††], Partha P. Jana*[†]

[†]Department of Chemistry, IIT Kharagpur, Kharagpur-721302, India

[#]School of Physical Science, NISER Bhubneswar, Khurda 752050, India

[††]Department of Metallurgical Engg.and Materials Science, IIT Bombay, 400076, India

ppj@chem.iitkgp.ac.in

§ denotes equal contribution

Abstract:

Ultralow thermal conductivity draws great attention in a variety of fields of applications such as themoelectics, thermal barrier coating, etc. Herein, crystal structure and transport properties of Cu_4TiSe_4 is reported.Cu_4TiSe_4 is a unique example of a non-toxic and low-cost material that exhibits lattice ultra-low thermal conductivity of 0.19 W $m^{-1}K^{-1}$ at room temperature. The main contribution to the unusually low thermal conductivity is connected with the atomic lattice and its dynamics. This ultralow value of lattice thermal conductivity (k_L) can be attributed to the presence of the localized modes of Cu which partially hybridized with the Se atoms, which in turn leads to avoid crossing of acoustic phonon modes that reaches the zone boundary with a reduced frequency. Like a phonon glass electron crystal, Cu_4TiSe_4 could also open the route for the finding of efficient thermoelectric materials, even, with chalcogenides of relatively high electrical resistivity and a large band gap, providing that their structures offer a sublattice with lightly bound cations.

10.1002/anie.202014222

Introduction:

In every energy conversion processes, certain percentage of heat is always liberated as universal by-product and mechanical work is one of the major source of energy dissipation. The unutilized heat waste could be effectively minimised by using thermal barrier coatings and refractories **[1]** or could be converted to electrical energy with the aid of efficient thermoelectric materials **[2-5]**. Therefore, continued search for new crystalline solid materials that can deliberately block the transportation of heat by virtue of their ultralow thermal conductivity (k) is underway.

Phonons and free charges are the routine carriers of heat in crystalline solids except in lead halide perovskites**[6],** where the photo generated hot charge carriers intrinsically inhibit the phonon propagation during cooling. The leading contribution to the thermal conductivity is generally connected with the atomic lattice and its dynamics. The lattice thermal conductivity (k_L) is formulated as $k_L = 1/3C_v vl$ within the frame work of kinetic theory, where C_v, v and l represent the specific heat at constant volume, group velocity of phonon and the phonon mean free path, respectively. In general, reduced k_L is achieved by two ways. Materials can be modified extrinsically by introducing point defect by incorporating foreign elements at the interstitial or lattice sites though the formation of solid solution. Another way is the modification of structural parameters (e.g; strains) intrinsically by altering the particles size which is directly related to lattice dynamics. All these strategies reduce the phonon relaxation time and hinder heat flow.

The compounds like clathrates **[7]** and skutterudites **[8]** could hold guest atoms into the cage-like structural voids, which substantially lower the k_L with low frequency rattling-like motion of the guest atoms. In the "phonon glass-electron crystal (PGEC)" compounds such as Cu_2Se**[9],**

Cu_3SbSe_3 **[10],** $AgCrSe_2$ **[11],** and AgCuX (X = S, Se, and Te) **[12],** liquid-like movement of cations also causes lowering of k_L.

Cu-based chalcogenides materials (in bulk) have been extensively investigated for the application of thermoelectric **[13–24]** and photo-voltaic **[25–29]** over the past few years. High natural abundance, low cost of Cu and chalcogens (e.g. S, Se) and suitable band gaps have made them very attractive candidates for photovoltaic applications.

Considering the importance of low-cost, high-performance materials for sustainable energy applications, the investigations are pursued in the copper-metal-chalcogenides (CMC) system. In this research program, Cu-Ti-Ch (Ch = Chalcogen) ternary system is the subject of our investigation. A literature survey reveals that the Cu_4TiS_4 and Cu_2TiTe_3 were structurally studied by Klepp *et al.***[30]** and Keane *et al.***[31]**. But there was no Se based compound reported in the ternary Ti-Cu-Se system when the investigation was initiated. In the recent past, a report describing the existence of Cu_4TiSe_4 has been published, which is focused on the crystal structure of the compound and has revealed its potential as a promising light-absorber in solar cells application. According to the report, the room temperature structure of Cu_4TiSe_4 (Table S1) was solved in a centrosymmetric space group $F\bar{4}3c$(219) with a lattice constant, a = 11.2936 (2) Å **[32]**. The structure contains 72 atoms per cell and has been reported as a $(2a)^3$ – superstructure of sulvanite (Cu_3MS_4, M=V, Nb, Ta).

The current investigation includes the synthesis, crystal structure and transport properties of Cu_4TiSe_4. The ternary compound has been synthesized from the highly pure constituent elements by high-temperature solid-state synthesis. The crystal structure has been studied by means of single-crystal X-ray diffractometry and energy dispersive X-ray diffraction analysis (EDX). The

structure model in this investigation differs from the previously reported model by Erica M. Chen *et al*. Our investigation shows that the structure adopts, Cu_3VS_4 ($P\bar{4}3m$; *cP*8, a=5.39 (1) Å), instead of its superlattice. The thermal conductivity of disordered Cu_4TiSe_4 is found to be as small as 0.19 W m^{-1} K^{-1}, a factor of 12 smaller than the thermal conductivity of CuSe and factor of 3 smaller than Cu_2Se at room temperature. This is probably the first ternary compound among CMC **[33-38]** and binary copper-chalcogenide with the lowest thermal conductivity at room temperature. Both experiment and computer simulation were employed to understand the ultralow thermal conductivity in this crystalline solid.

Experimental Section:

Synthesis.

The samples were prepared by high-temperature solid-state synthesis from highly pure constituent elements (Ti powder, 99.99%; Cu ingot, 99.99%; Se powder,99.999%). Initially elemental Ti, Cu, and Se were taken approximately in the ratio of 1:2:3 in a quartz tube and the tube was sealed under vacuum (about 10^{-5} mbar). The ampoule was heated at a temperature of 900°C with a rate of 180°C/hour, annealed at this temperature for 120 hours and then slowly cooled down to 300°C over a period of the 96 hours and then allowed to cool to room temperature. The black coloured crystals were obtained from the crushed ingot. The crystals were mechanically separated, were analysed compositionally by Energy Dispersive X-ray Spectroscopic (EDX) technique and it showed the approximate composition of Cu_4TiSe_4. Subsequently, a series of samples were synthesised according to the EDX composition. To improve the quality of single crystal for structural characterisation, the samples were further annealed at 900°C for the period of 100 hours

10.1002/anie.202014222

and finally cooled down to 200°C at a rate of 6°C/hour. However, phase pure polycrystalline samples were prepared following the temperature program used by Erica M. Chen *et al*.**[32]**.

Single Crystal X-ray diffraction data collection and processing.

The single crystals (C1, C2, and C3) were mechanically separated from the crushed ingot and picked on a glass slide. The cuboid crystals of approx. dimensions ~0.2 mm were picked on the tip of the glass fibre by tiny amount of glue and mounted on goniometer head. The diffraction intensities were collected on BRUKER D8 VENTURE with PHOTON II detector equipped with graphite-monochromatic Mo-target Kα radiation (λ = 0.71073 Å) at ambient temperature. Data collection, reciprocal space construction, and data reduction were performed Apex III software and CrysAlis Pro. The structure solution and the structure refinement were carried out using the *Jana2006* program **[39-40]**. The reflections were indexed on the basis of a ~5.6 Å primitive cubic unit cell **[Fig. 1]** for the room temperature dataset.

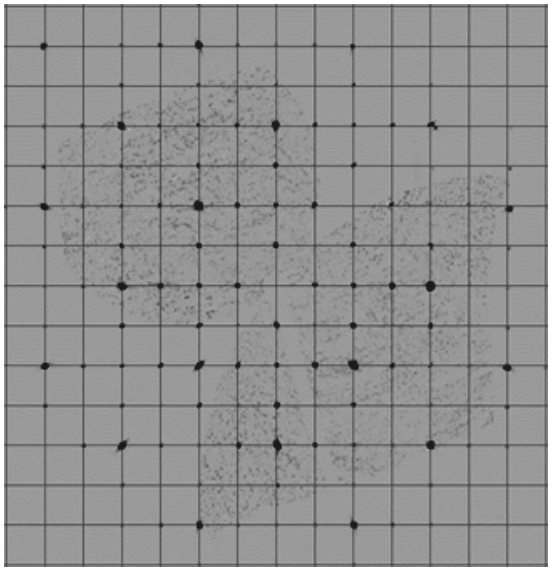

Fig.1*. A reciprocal space view (hk0) of a cubic unit cell with a lattice parameter of a=5.6458(1) Å. Single lattice is clearly visible (black) without any superstructure reflection.*

It is worth mentioning that the diffraction data collected on Cu_4TiSe_4 were thoroughly checked, and there is absolutely zero indication of Bragg reflections in (hk½) and (hk3/2), which suggest there is no cell doubling, or otherwise any diffuse scattering (supporting information Fig. S1).

Powder X-ray diffraction data collection.

To confirm the purity, analyse the adjacent phases, and to identify new phases**,** X-ray powder diffraction experiments were performed for all the synthesised samples. Ingots were crushed and thoroughly ground into powder with agate mortar and pestle. Powder X-ray diffraction data were collected at room temperature by using BRUKER D2 PHASER diffractometer with Cu-Kα X-ray radiation (λ=1.5418Å). Data measurement was carried out with a step size of 0.02°. The powder diffraction data of the prepared samples were analysed by Rietveld refinement using *Jana2006* program.

Field emission scanning electron microscopy (FE-SEM) and energy dispersive X-ray spectroscopic analysis (EDX).

Black coloured selected crystals from the crushed ingot were subjected for chemical analysis in a Nova Nano SEM 450 field emission scanning electron microscope (FE-SEM) equipped with Bruker energy dispersive X-ray analyser (EDX). EDX data were acquired with an accelerating voltage of 10-15 kV and an accumulation time of the 50s.

Pallet Preparation.

A pallet was made from a phase pure finely powdered sample under a pressure of 50 MPa at 573K by Spark Plasma Sintering (SPS) technique. Sample was sintered at this temperature and pressure for 10 minutes.

Physical property measurement.

Thermal conductivity, electrical resistivity and heat capacity were measured in Quantum Design PPMS at low temperature.Diffuse reflectance spetroscopic measurement was carried out in a Varian Cary 5000UV-Vis-NIR spectrometer in the wavelength ranging 200nm to 2000nm.

Computational details:

The first principle calculations were carried out to analyze the electronic structure and transport properties of Cu_4TiSe_4 within the framework of density functional theory (DFT) **[41-42]**. The calculations were performed using Vienna ab-initio simulation package (VASP) **[43]**, which is a plane wave based electronic structure code. The Generalized Gradient Approximation (GGA) **[44]** with Perdew-Burke-Ernzerhof (PBE) formulation was used to treat the electronic exchange and correlation. A plane-wave cutoff energy of 550 eV and an energy convergence criterion of 10^{-4} eV were used. Convergence in energy was checked with respect to K-mesh size and a 15x15x15 K-mesh was employed for the conventional cell with nine atoms. In all cases, ionic as well as geometric relaxations were performed.

The phonon band structure was calculated using the finite displacement method as implemented in the phonopy **[45]** code. Converged supercell of 2x2x2 was used to calculate the phonon band structure. The amplitude of the displacements was fixed to 0.01 Å, and the forces were converged

to the accuracy of 10^{-8} eV/ Å. The phonon group velocity υ ($\upsilon = \frac{\mathrm{d}\omega}{dK}$), mode resolved phonon group velocity υ_i($\upsilon_i = \frac{\mathrm{d}\omega_i}{dK}$), Grüneisen parameter γ ($\gamma = \frac{-V_0}{\omega}\frac{d\omega}{dV}$), and mode resolved Grüneisen parameter $\gamma_i\left(\gamma_i = \frac{-V_0}{\omega_i}\frac{d\omega_i}{dV}\right)$ were extracted from the harmonic phonon band dispersion using self-written python based extensions to phonopy-VASP. For calculating the γ and γ_i, the lattice was subjected to biaxial strains of ±2 %. Finally, the Asen-Palmer modified version of the Debye Callaway theory parametrized for solid **[46]** was used to calculate lattice thermal conductivity (k_L) of the compounds (which is provided in the supplementary material).

Result and discussions:

Structure solution, refinement and phase analysis.

The structure solution were carried outby *Superflip* **[39]**, which is implemented with *Jana2006*. Structural refinements were performed in *Jana2006* software package **[40]**. Superflip is used only to create the original model whilst *Jana*2006 is used for the refinement. The refinement is a standard least squares refinement of the positions and displacement parameters of the atoms. The structure solution of C1 yielded three crystallographically independent sites in the unit cell, out of them, one is selenium site (Se1; 4e), one is titanium site(Ti1; 1b) and another one is Cu site (Cu1; 3c). At this stage, the preliminary structure refinement converged at R(F) of 11%. An additional atomic position (4*e*) at x ≈0.83 and y = z ≈ 0.17 was identified in residual electron density maps and included as copper (Cu2). The structural model was refined. Cu2 site showed relatively large atomic displacement parameter. Hence, this particular site was checked for partial occupancy, and subsequent refinement resulted in the residual value of 10%. An additional site (1a) at (0, 0, 0) was further identified in residual electron density map and assigned as copper (Cu3). The distance

between Cu2 site and Cu3 was too short (~1.52 Å). Hence, Cu3 site was checked for partial occupancy. The structural model was refined and subsequent refinement resulted in the residual value of ~8%. Cu2 and Cu3 split into five positions [one at (0, 0, 0) and four at 4e;x ≈ 0.83, y = z ≈ 0.17]. At (0, 0, 0) site occupancy factor (SOF) of Cu is ~0.34 and SOF of Cu at each 4e site is ~ 0.16. The correlation between the independently refined occupations factors kept the total occupancy of disordered Cu sites (4xSOF(Cu2) +SOF(Cu3)) close to unity **[Fig. 2]**. It is worthy to mention that positional disorder in copper site was previously found in copper-based chalcogenides (e.g. Cu_4MS_4 (M= Ge, Sn)) **[47]**. Harmonic ADPs of the atoms were taken into account for all including the positionally disordered sites.

This model was used as a starting model for the refinement of single-crystal X-ray diffraction data collected for compound C2 and C3. The final refinement including an isotopic extinction correction yielded $R(F^2)$ ($F^2>3\sigma(F^2)$) values between 3% and 4% **[Table S2]**. Measurement details and refinement results are mentioned in **Table S2**. The atomic coordinates together with their site occupancy and thermal displacement parameters are listed in **Table S3**.

SCXRD data refinement gave a composition close to that of composition received from EDX analysis **[Table S2]**. For physical property measurement, the phase pure samples were prepared by using the temperature program according to previous report by Erica M. Chen *et al.***[Fig. S2].** Phase analysis was performed with different loaded composition [**Table S3**] and no phase-width was observed for our reported compound(supporting information **Table S4**).

It is worth to mention that Erica M. Chen *et al.* [**Fig. S3**] have used a larger unit cell with a lattice constant, a = 11.2936 (2) Å to describe the structure of Cu_4TiSe_4. The structural model, which was refined in the space group $F\bar{4}3c$ (219), contains 72 atoms. The atoms are distributed only at high

10.1002/anie.202014222

symmetry sites (32e, 24d, 8a and 8b), and, in standard settings, it must be described by the space group $P\bar{4}3m$ with the unit cell parameter a=5.6468 Å, the same as what we find for our structure (Supporting information Fig. S3, SI1). Thus, it is concluded that the reported crystal structure *by Chen et al.*was incorrect. Moreover, the large atomic displacement parameters in a position (¼, ¼, ¼) suggests that they have erroneously assigned Ti atom (Table S0) in their proposed structural model.

Crystal Structure.

The crystal structure of Cu_4TiSe_4 is closely related to mineral sulvanite, Cu_3VS_4 ($P\bar{4}3m$; *cP*8, a=5.39 (1) Å) **[33]** and Cu_4TiS_4 (*tI*18; $I\bar{4}2m$ (121), a = 5.448(1) Å c = 10.565(2) Å) **[Fig S4] [30]**.

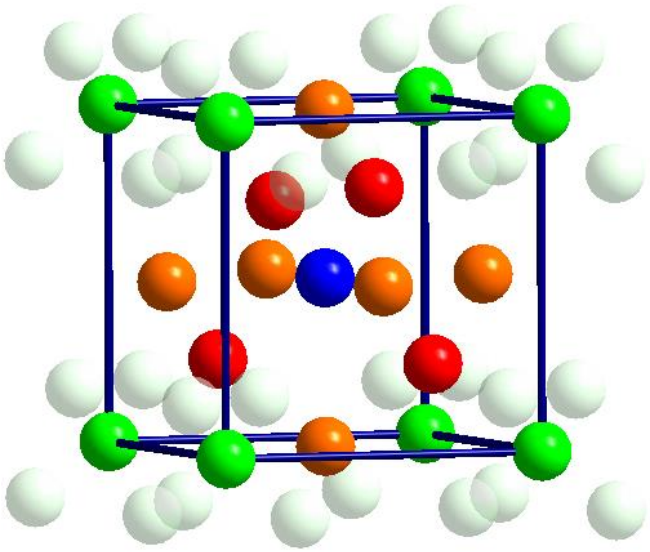

Fig. 2. *Unit cell of Cu_4TiSe_4 placing Ti site at the centre of the unit cell. Ti, and Se atoms are represented by blue, and red coloured spheres, respectively. Four fold split copper sites (Cu2) around Cu3 (0,0,0) are shown. Cu1, Cu2 and Cu3 are represented in orange, light green and deep green color, respectivey.*

Optical band gap determination using UV-Vis-NIR spectroscopy.

From the reflectance value, the Schuster–Kubelka–Munk function (F_{SKM}) can be calculated**[48]** as:

$$F(R) = \frac{(1-R)^2}{2R}$$

Where, R= reflectance (% of R/100). Now, as F(R) is proportional to the optical absorption coefficient (α) **[48]**, so Tauc equation **[49]** can be used for the analysis:

$$(\alpha h\nu)^{1/n} = A(h\nu - E_g)$$

The above equation can be written in terms of F(R) as:

$$[\mathrm{F(R)}h\nu]^{1/n} = A(h\nu - E_g)$$

where, h is Planck's constant, ν is the frequency of radiation, A is a constant, E_g is optical bandgap and the value of 'n' denotes the nature of the electronic transitions. n =1/2 corresponds to direct allowed transition (then $E_g = E_g^{dir}$= direct bandgap energy) and n=2 corresponds to indirect allowed transition (then $E_g = E_g^{indir}$= indirect bandgap energy). From the extrapolation of $(\alpha h\nu)^{1/n}$ versus $h\nu$ curves to $(\alpha h\nu)^{1/n}$= 0, the value of E_g^{dir} and E_g^{indir} were determined 1.59 eV and 1.42 eV **[Fig.3]** respectively at 300 K temperature. Therefore, the compound is a wide bandgap semiconductor for room temperature applications. The optical band gap of this compound is comparable to the fundamental electronic band gap.

10.1002/anie.202014222

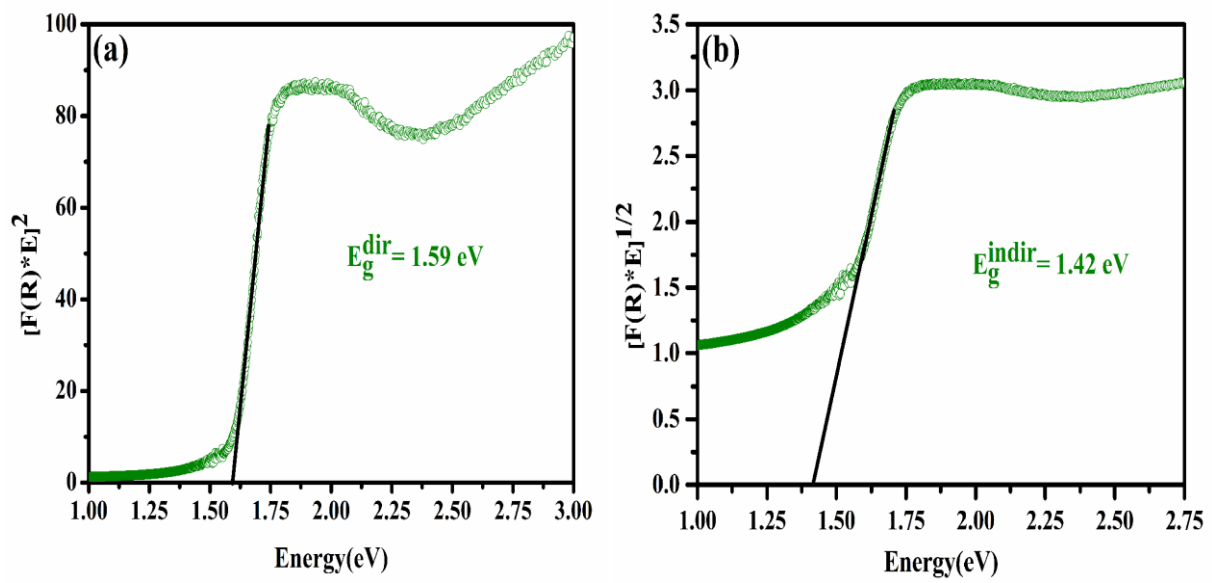

Fig.3.*Tauc plots for optical band gap measurements showing* ***a)*** *direct bandgap and* ***b)*** *indirect bandgap of* Cu_4TiSe_4.

Thermal and electrical conductivity.

Figure 4(left) represents the temperature dependence of the thermal conductivity of Cu_4TiSe_4. At room temperature, total thermal conductivity (k_T) was found to be extreme low (0.19 $W \cdot m^{-1}.K^{-1}$). The value at room temperature is much lower compared to the Cu_2Se **[Fig. 5]**. On moving to lower temperature the conductivity increases and there is a sudden increase in the value (from 0.36 $W \cdot m^{-1}.K^{-1}$to 0.43 $W \cdot m^{-1}.K^{-1}$) at temperature 180K which is due to phase transformation. It is further confirmed by heat capacity measurement **[Fig. S5]**.

10.1002/anie.202014222

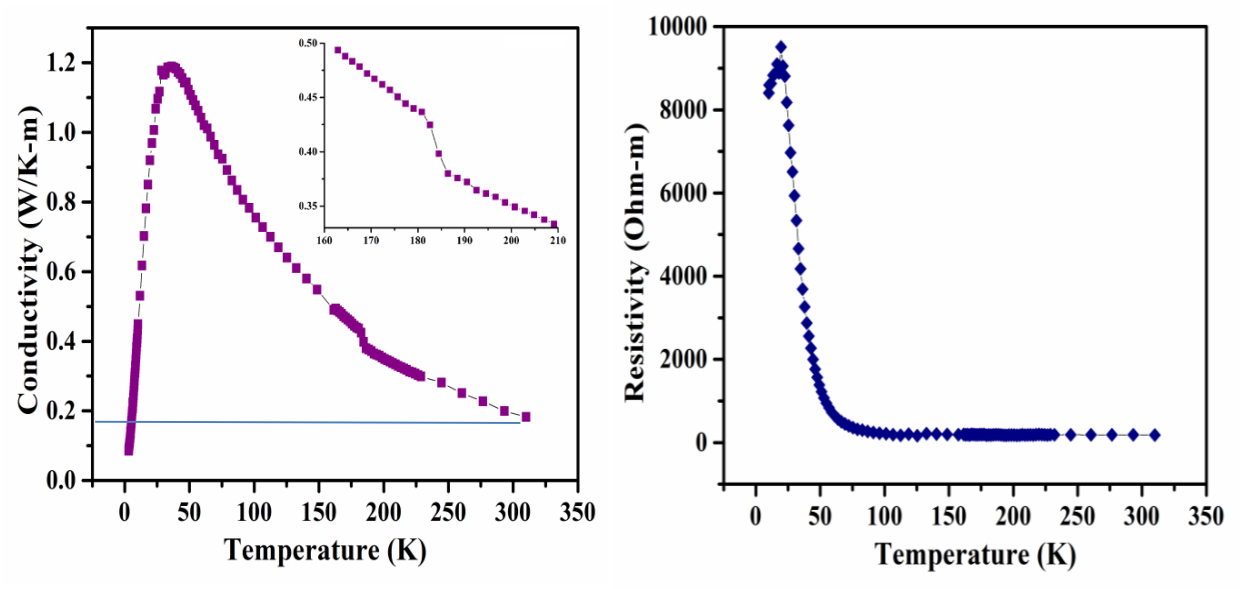

Fig.4 (left) *Thermal conductivity vs temperature plot;* ***(right)*** *Resistivity vs temperature plot for phase pure* Cu_4TiSe_4 *sample within the temperature range (4K to 310K).*

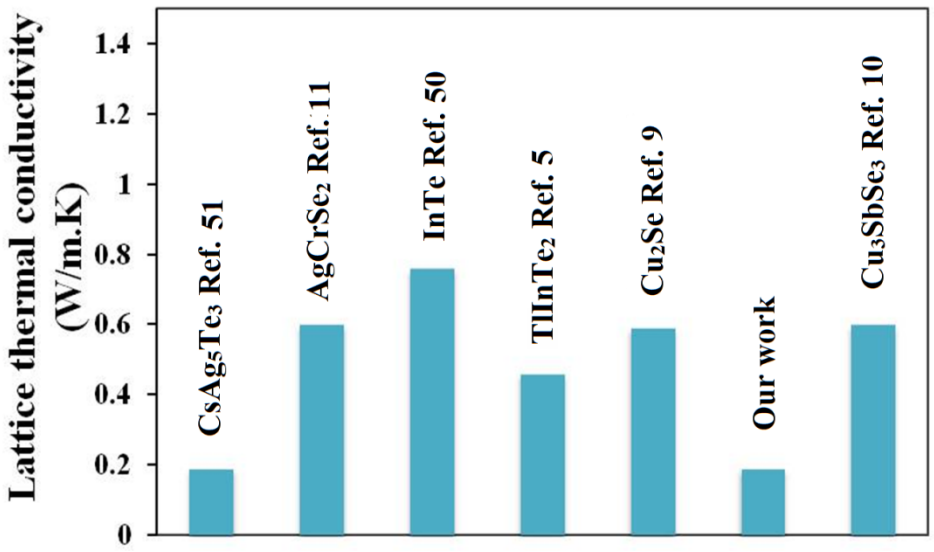

Fig.5*. Summary of the materials with ultra-low thermal conductivity at room temperature.*

Thermal conductivity sharply increases with further lowering of temperature and reach to maxima at ~50K, then drop too steeply to 0.08 $W \cdot m^{-1}.K^{-1}$at 4K **[Fig. 4]**. The measured electrical resistivity was used to extract electronic thermal conductivity (k_{el}) with the help of the Wiedemann–Franz law.Thereafter, k_L is obtained from k_T by deducting k_{el} as k_T is combination of k_L and k_{el}. Since the compound is electrically insulating **[Fig. 4]** in nature, the measured thermal conductivity is k_L.

Heat Capacity.

To get further insight, the heat capacity was measured between 2 and 300 K but data ranging from 2-55K was shown in the plot of Cp/T vs. T^2 **[Fig. 6].** The complete dataset ranging from 2-300K has been modelled using the combined Debye-Einstein model as following Eq:

$$\frac{C_p}{T} = \gamma + \beta T^2 + \sum_n \left(A_n (\Theta_{E_n})^2 \cdot (T^2)^{-3/2} \cdot \frac{e^{\Theta_{E_n}/T}}{(e^{\Theta_{E_n}/T} - 1)^2} \right)$$

In this equation, electronic contribution is introduced by ɣ and Debye mode contribution by βT^2 , where $\beta = C.(12\pi^4 N_A k_B/5).(\theta_D)^{-3}$ with N_A, k_B, θ_D being the Avogadro number, Boltzmann constant and Debye temperature, respectively. The parameter C is given as $C = 1 - \sum_n A_n/(3NR)$, where N is the number of atoms per formula unit and R is the universal gas constant. The Debye temperature (θ_D) for the compound is estimated to be 204 K from the value of β. Three Einstein modes are estimated after modelling the temperature dependence through the fitting to whose characteristic temperatures to be 35.54K (θ_{E1} =24.7 cm^{-1}), 81.01K (θ_{E2} =56.3 cm^{-1}) and 179. 24K (θ_{E3} =124.6 cm^{-1}; **Table S4**). The Einstein modes represent quasi-localized optical phonon modes arising from the vibrations of weakly bound atoms. Contribution to Cp at low temperatures is dominated by low-energy optical modes,which manifest as the Einstein oscillators. These low-

energy optical modes scatter the heat-carrying acoustic phonons thereby deteriorating the phonon transport of heat.

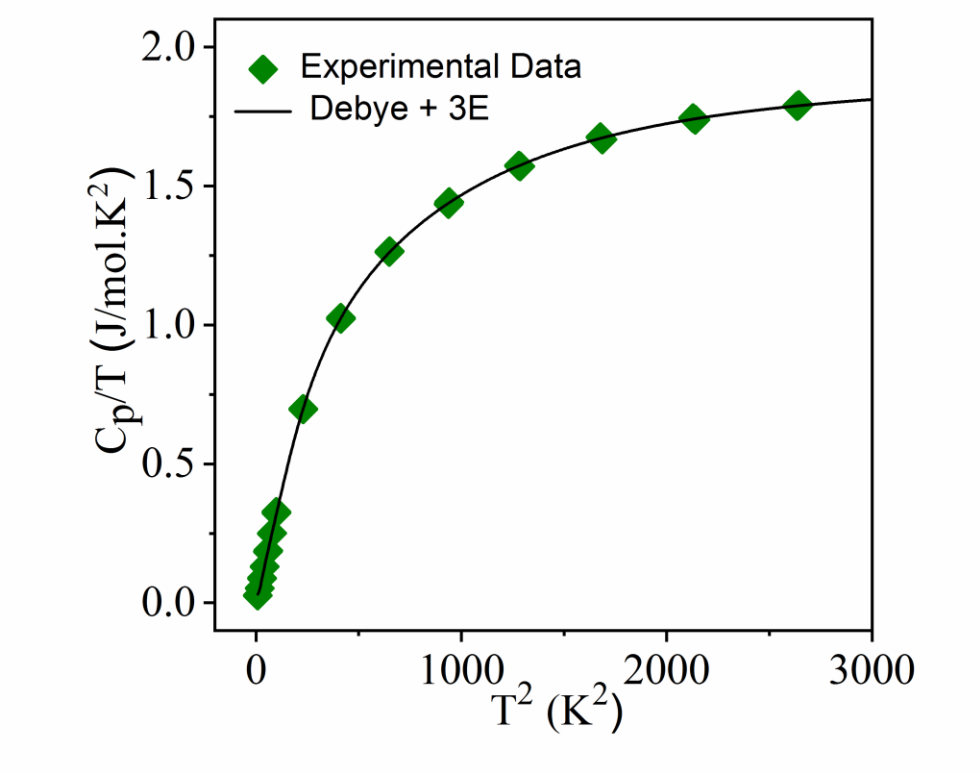

Fig.6 *C_p/T vs T^2 plot.*

Electronic and phonon dispersion of the ordered supercell (SI2**) from the disordered structure**

The first principles density functional theory based calculations **[Fig. 7]** have been employed to calculate electronic structure of the supercell generated from disordered structure (SI2-a, Table S5, Fig. S6) using the GGA PBE XC functional. The electronic band structure of Cu_4TiSe_4 is plotted along the high symmetry path Γ-X-M-Γ-R-X in the irreducible part of the first Brillouin zone corresponding to the face-centered cubic lattice, which shows an indirect band gap (E_g = ~0.9 eV), between the M (valence band maxima, VBM) and Γ (conduction band minima, CBm) point as shown in **Fig. 7(a)**. The conduction bands and valence bands near the Fermi level are majorly

10.1002/anie.202014222

contributed by the Cu-dand Ti-d statesas can be seen from the partial electronic contribution of the specific atoms in the density of states.The electronical band structure calculation is validated using the meta-GGA functional, which gave a similar trend of indirect band gap between the M (VBM) and Γ (CBm) point in the band structure. However, the magnitude band gap of 1.2 eV, is found to be ~ 25 % higher than the usually underestimated GGA band gap (see SI **Fig. S7**). In order to explore the effect of localized d electrons in the band gap, the calculations (GGA+U) were performed by incorporating the Hubbard U in the Hamiltonian (see SI, **Fig. S9**). The magnitude, the trend, and the elemental contributions in the CBm were found to be similar to the one calculated using meta GGA.

Except for the well known band gap estimation problem, no other noticeable change in bonding chemistry (viz. from the elemental contribution in VBM or CBm etc) was observed for the PBE GGA. Thus, PBE GGA was employed for performing the computationally demanding phonon calculations. The corresponding phonon band structure of the structure (of the converged 1X1X1 structure) is given in **Fig. 7(b)**. It shows the presence of imaginary acoustic phonon modes along the Γ-R-X direction of the dispersion, which in turn suggest towards dynamically instable mode of vibrations. Thus, the presence of the instability in the structure prevents the use of Debye-Callaway or equivalent models for estimating the lattice thermal conductivity.

10.1002/anie.202014222

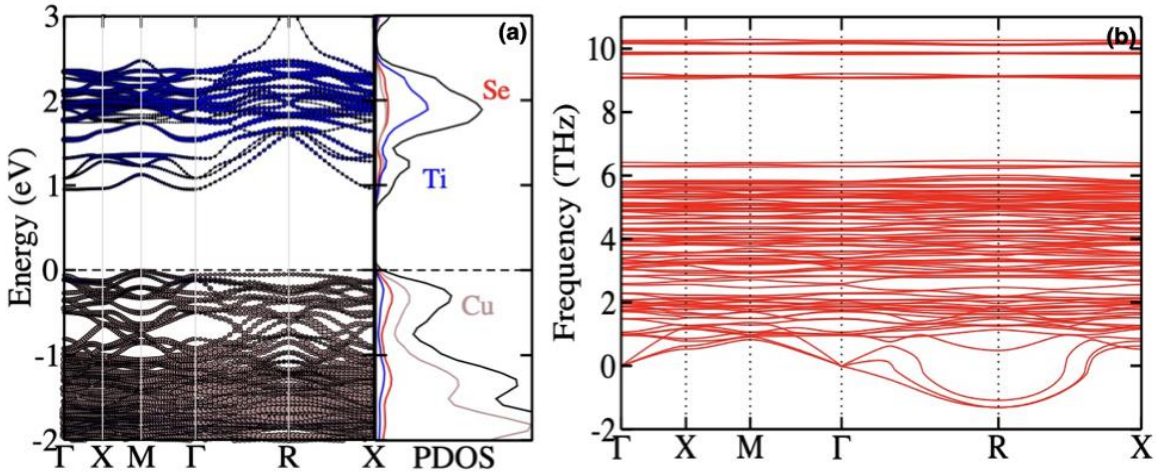

Fig.7 a)*. Electronic band dispersion and atom projected (coloured)/ total density of states (black),* ***b)*** *phonon band dispersion of the supercell (2x2x1)generated from the disordered* Cu_4TiSe_4 *structure.*

Electronic and phonon dispersion of the ordered structure with original cell (1×1×1).

In order to get an idea of the lattice thermal conductivity a disorder free lattice is considered. The disorder free (SI2-b), structure of Cu_4TiSe_4 comprises of nine atoms (with four Cu, four Se and one Ti) in one unit cell with a cubic structure with lattice parameter of 5.6 Å. This ground state configuration of Cu_4TiSe_4 exists in the space group $P\bar{4}3m$ with different ions occupying different Wyckoff positions viz. Cu [1a (0, 0, 0) and 3c (0.5, 0, 0.5)], Se [4e (0.23967, 0.23967, 0.23967)], and Ti [1b (0.5, 0.5, 0.5)]. The symmetry unique Cu-1a (green) and Cu-3c (orange) form the face-centered lattice, whereby half of the tetrahedral voids (alternate) are occupied by 4 Se atoms (red) and the center of the cube is occupied by a Ti atom (blue) **[Fig. 2]**. The electronic band structure of the ordered Cu_4TiSe_4 show an indirect band gap of E_g = ~1.2 eV as shown in **Fig. 8(a)**.The corresponding discussion of the effect of the XC functional in the electronic band structure is provided as the supplementary information (see SI **Fig.S8**). The detailed phonon calculations are

performed on the stable ground state ordered structure. A convergence in the phonon density of states was reached for 2X2X2 supercell [see SI **Fig. S10**]. The converged phonon band structure and phonon partial density of states (PhDOSs) of the ordered Cu_4TiSe_4 are shown in **Fig. 8(b)**, whereby the acoustic phonon modes are shown in dotted lines. It should be noted that the acoustic modes have low Debye cut off frequency (i.e. the frequency with which the modes reach the Brillouin zone boundary), since it is limited by the avoided crossing occurring due to the presence of the localized flat bands (shown in cyan) in the phonon band structure. As seen from the PhDOS presented in the middle panel of **Fig. 8(b),** the localized modes of Cu-3c (orange) and Cu-1a (green) atoms equally contribute to the flat bands. However, these modes are not completely isolated 'rattling' modes, since they have slight dispersion or spread, which is due to the partial hybridization with Se-4e atom (as seen from the individual atomic contributions from phonon partial density of states). As seen from the last panel of **Fig. 8(b)**, the first peak due to the hybridization between the Cu-3c and Se-4e occurs at 1.4 THz (46.7 cm^{-1}), while a second peak is observed at 2.0 THz(66.72 cm^{-1}),which is due to the hybridization between the Cu-1a and Se-4e atoms. The mode resolved (υ_i) and average (υ_s) (calculated as $\left[\frac{1}{3}\left(\left(\frac{1}{\upsilon LA^3}+\frac{1}{\upsilon TA^3}+\frac{1}{\upsilon TA'^3}\right)\right)\right]^{\frac{-1}{3}}$) phonon group velocity (Km/s), mode resolved Gruneisen parameter (γ_i) and Debye temperature (θ_D) of the TA and LA branches as calculated from the phonon dispersion are enlisted in **Table 1** and shown in **Fig. 8(c)** and **(d)** respectively. υ_i and γ_i are calculated from the average of group velocity and Gruneisen parameter attained by the modes originating from the Γ point in various direction of the Brillouin zone. Finally, the k_L is calculated by modelling the phonon scattering lifetime using the Debye Callaway formalism of solid. The temperature dependency of the lattice thermal conductivity computed for Cu_4TiSe_4 is shown in **Fig. 8(e).** As the temperature increases anharmonicity increases and therefore the lattice thermal conductivity decreases. At 300 K, k_L of

10.1002/anie.202014222

Cu_4TiSe_4 found to be 0.12 $Wm^{-1}K^{-1}$, which is fairly in agreement to the experimental value. This ultralow value of k_L can be attributed to the presence of the localized modes of Cu which was also partially dispersed due to their hybridization with the Se atoms. This, in turn leads to avoided crossing of acoustic phonon modes, which reach the zone boundary with a reduced frequency. Although the k_L of supercell model generated from the experimental disordered structure has not been calculated theoretically explicitly, but a close analogy can be drawn between the k_L of the two structures. The acoustic phonon modes in the supercell model of the disordered structure reach the zone boundary at much lower frequency (by 40 %) than the corresponding ones in the ordered structure (which is the estimation of the Debye temperature, θ_D). Moreover, all the optical phonon modes in the supercell model (2x2x1) of the disordered structure is composed majorly of flat bands, which implies zero group velocity (hence, no contribution to the k_L). Thus, low θ_Ds and flat optical phonon dispersion in the supercell model of the disordered structure suggests that the $k_L$of the disordered structure will be even lower than the ordered structure which has been currently analyzed.

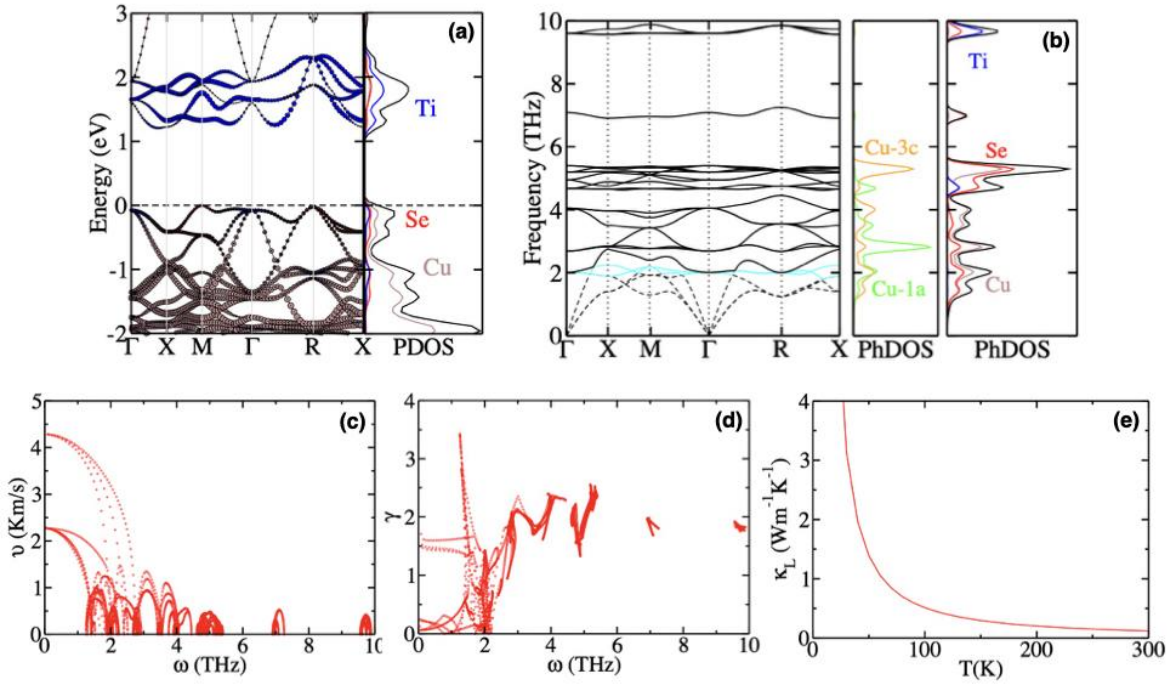

Fig.8. a) *The electronic band structure of the ordered Cu_4TiSe_4 (Cu (1a and 3c-brown), Se (4e-red) and Ti (1b-blue) atoms) with original cell,* ***b)****Phonon band structure (left panel) and partial density of states of the ordered Cu_4TiSe_4 (right panel). Projected density of states of the symmetrically unique copper atoms, Cu-1aand Cu-3c (middle panel),* ***c)*** *The acoustic group velocity (υ),* ***d)****Grunesien parameter (γ) plotted as a function of frequency (ω), and* ***e)*** *The lattice thermal conductivity k_L calculated using Debye Callaway formalism.*

Table 1. The mode resolved (υ_i) and average (υ_s) phonon group velocity (Km/s), mode resolved Grunesien parameter (γ_i) and Debye temperature (θ_D) of the TA and LA branches. $\boldsymbol{k_L|_{300}}$ denotes the lattice thermal conductivity at 300 K.

System	υ_i	υ_s	γ_i	$\Theta_D k_L\|_{300}$	
	υ_{TA}1.9		γ_{TA}6.0	θ_{TA}64	
Cu_4TiSe_4	υ_{TA}, 1.9	2.1	γ_{TA}, 6.0	θ_{TA}, 74	0.12
	υ_{LA}3.5		γ_{LA}4.0	θ_{LA}86	

Conclusion:

Recently discovered ternary copper titanium selenide Cu_4TiSe_4 has been reinvestigated in this report. In contrast to previous report, Cu_4TiSe_4 crystallizes centrosymmetric space group $P\bar{4}3m$ (*cP*9) and adopts Cu_3VSe_4 structure (*cP*8) type with an additional Cu site at (0 0 0). No evidence of superlattice is observed in the room temperature X-ray diffraction experiment. The room temperature structure displays positional disorder at copper sites, which is different finding from the previous report. Cu_4TiSe_4 display high optical band gap of ~1.50 eV.The compound shows

surprisingly high electrical resistivity in the order of 10^2 at room temperature. At room temperature, total thermal conductivity (k_T) was found to be as low as 0.19 $W \cdot m^{-1}.K^{-1}$. This major achievement results from strong optical-acoustic coupling with low cutoff frequencies and a rigid covalent bonding framework of Ti-Se interlocked with weakly bound ionic substructure comprising of Cu^+ cations (intrinsic rattlers) which allows a thermal conductivity similar to that of a glass to be reached. Cu_4TiSe_4 may have significant implications both in the field of thermal coating materials and solar cell absorber due to its nontoxicity and fabrication from the low cost earth abundant elements. Like phonon glass electron crystal, Cu_4TiSe_4 with the ultra-low value of k_L, could also open the route for the discovery of efficient thermoelectric materials. Even, compound especially chalcogenides with relatively high electrical resistivity and large band gap deserve to be revisited, providing that their structures offer a sublattice with lightly bound cations.

Acknowledgment:

The authors would like to thank the Science & Engineering Research Board (SERB), India for Early Career Research Award. BK acknowledges UGC for fellowship.BK would like to thank Dr.Ajay Nayek for allowing data collection, Paribesh Acharyya for his help in preparation of C_p/T vs T^2 plot. AB acknowledges the DST Inspire faculty fellowship and Early Career Research award by SERB India.

Author contributions

B.K. synthesized the samples, carried out structural characterization, model preparation form electronic structure calculation, performed data analysis, and wrote the maximum part ofmanuscript. A. L. synthesized the samples, performed DRS measurement and co-wrote the manuscript. P.R.R. and A.B. (IIT Bombay) performed calculations of electronic structure and phonon dispersion,wrote that section of manuscript. C. S. (NISER, Bhubaneshwar) measured

thermal conductivity, electrical resistivity, heat capacity and helped to draw those pictures. P.P.J. conceived and supervised the entire project, performed crystal structure measurement, and structure determination helped to analyse the results and co-wrote the manuscsript.

Reference:

[1] N. P. Padture,M. Gell, E. H. Jordan, *Science*, **2002**, *296*, 280.

[2] L. D. Zhao, V. P. Dravid, M. G. Kanatzidis, *Energy Environ. Sci.*, **2014**, *7*, 251−268.

[3] a)C. Chang, M. Wu, D. He, Y. Pei, C.-F. Wu, X. Wu, H. Yu, F. Zhu, K. Wang, Y. Chen, L. Huang, J.-F. Li, J. He, L. D. Zhao, *Science*, **2018**, *360*, 778; b) L. D. Zhao, S. H. Lo, Y. Zhang, H. Sun, G. Tan, C. Uher, C. Wolverton, V. P. Dravid, M. G. Kanatzidis, *Nature*, **2014**, *508 (7496)*, 373−7; c) G. Tan, L. D. Zhao, F. Shi, J. W. Doak, S. H. Lo, H. Sun, C. Wolverton, V. P. Dravid, C. Uher, M. G. Kanatzidis, *J. Am. Chem. Soc.***2014**, *136 (19)*, 7006−17; d)S. Roychowdhury, R. K. Biswas, M. Dutta, S. K. Pati, K. Biswas, *ACS Energy Lett.*, **2019**, *4*, 1658.

[4] a) M. Samanta, T. Ghosh, R. Arora, U. V. Waghmare, K. Biswas, *J. Am. Chem. Soc.*, **2019**, *141*, 19505.b) M. K. Jana, K. Pal, A. Warankar, P. Mandal, U. V. Waghmare, K..Biswas,*J. Am. Chem. Soc.***2017**, *139*, 4350−4353.

[5] S. Mukhopadhyay, D. S. Parker, B. C. Sales, A. A. Puretzky, M. A. McGuire, L. Lindsay, *Science*, **2018**, *360*, 1455.

[6] J. Yang, X. Wen, H. Xia, R. Sheng, Q. Ma, J. Kim, P. Tapping, T. Harada, T. W. Kee, F. Huang, Y. Cheng, M. Green, A. Ho-Baillie, S. Huang, S. Shrestha, R. Patterson, G. Conibeer *Nat. Comm.*, **2017**, *8* (1), 1-9.

[7] T. Takabatake, K. Suekuni, T. Nakayama, E. Kaneshita, *Rev. Mod. Phys.* **2014**, *86*, 669−716.

[8] X. Shi, J. Yang, J. R. Salvador, M. Chi, J. Y. Cho, H. Wang, S. Bai, J. Yang, W. Zhang, L. Chen, *J. Am. Chem. Soc.***2011**, *133*, 7837−7846.

[9] H. Liu, X. Shi, F. Xu, L. Zhang, W. Zhang, L. Chen, Q. Li, C. Uher, T. Day, G.J. Snyder, *Nat. Mater.***2012**, *11*, 422–425.

[10] W. Qiu, L. Xi, P. Wei, X. Ke, J. Yang, W. Zhang, *Proc. Natl. Acad. Sci. U. S. A.* **2014**, *111*, 15031.

[11] B. Li, H. Wang, Y. Kawakita, Q. Zhang, M. Feygenson, H. L. Yu, D. Wu, K. Ohara, T. Kikuchi, K. Shibata, T. Yamada, X. K. Ning, Y. Chen, J. Q. He, D. Vaknin, R. Q. Wu, K. Nakajima, M. G. Kanatzidis, *Nat. Mater.* **2018**, *17*, 226−230.

[12] a) S. Ishiwata, Y. Shiomi, J. S. Lee, M. S. Bahramy, T. Suzuki, M. Uchida, R. Arita, Y. Taguchi, Y. Tokura, *Nat. Mater.,* **2013**, *12*, 512; b) S. Roychowdhury, M. K. Jana, J. Pan, S. N. Guin, D. Sanyal, U. V. Waghmare, K. Biswas, *Angew. Chem. Int. Ed.,* **2018**, *57*, 4043−4047.

[13] X. Y. Shi, F.Q. Huang, M.L. Liu, L.D. Chen, *Appl.Phys.Lett.,* **2009**, *94*, 122103.

[14] M. L. Liu, I.W. Chen, F.Q. Huang, L.D. Chen, *Adv. Mater.,* **2009**, *21,* 3808–3812.

[15] X. Y. Shi, L. L. Xi, J. Fan, W.Q. Zhang, L.D. Chen, *Chem. Mater.***2010**, *22*, 6029–6031.

[16] J.Y. Cho, X. Shi, J.R. Salvador, G.P. Meisner, J. Yang, H. Wang, A.A. Wereszczak,X.Zhou, C. Uher, *Phys. Rev. B.*, **2011**, *84*, 085207.

[17] E. J. Skoug, J. D. Cain, D. T. Morelli, *Appl. Phys. Lett.,* **2011**, *98*, 261911.

[18] T. Plirdpring, K. Kurosaki, A. Kosuga,T. Day, S.Firdosy, V. Ravi, G. J. Snyder, A. Harneunggmoung, T. Sugahara, Y. Ohishi, H. Muta, S. Yamanaka, *Adv. Mater.*, **2012**, *24*, 3622–3626.

[19] R. Liu, L. Xi, H. Liu, X. Shi, W. Zhang, L. Chen, *Chem. Commun.,* **2012**, *48*, 3818–3820.

[20] X. Lu, D. T. Morelli, Y. Xia, F. Zhou, V. Ozolins, H. Chi, X.Y. Zhou, C. Uher, *Adv.Energy Mater.,* **2013**, *3*, 342–348.

[21] K. Suekuni, K. Tsuruta, M. Kunii, H. Nishiate, E. Nishibori, S. Maki, M. Ohta, A. Yamamoto, M. Koyano, *J. Appl. Phys.*, **2013**, *113,* 043712.

[22] Y. Goto, Y. Kamihara, M. Matoba, *J. Electron Mater.*, **2014**, *43*, 2202–2205.

[23] A. Suzumura, N. Nagasako, Y. Kinoshita, M. Watanabe, T. Kita, R. Asahi, *Mater.Trans.*, **2015**, *56*, 858–863.

[24] J. Fan, W. Carrillo-Cabrera, L. Akselrud, I. Antonyshyn, L. Chen, Y. Grin, *Inorg. Chem.*, **2013**, *52*, 11067–11074.

[25] a) Q. Guo, G. M. Ford, W. C.Yang, B. C. Walker, E. A. Stach, H. W. Hillhouse, R. Agrawal, *J. Am. Chem. Soc.*, **2010**, *132*, 17384–17386; b) S. C. Riha, B. A. Parkinson, A. L. Prieto, *J. Am. Chem. Soc.*, **2009**, *131*, 12054–12055; c) S. C. Riha, B. A. Parkinson, A. L. Prieto, *J. Am. Chem. Soc.*, **2011,***133*, 15272–15275.

[26] a) D. B. Mitzi, O. Gunawan, T. K. Todorov, K. Wang, S. Guha, *Energy Mater.Sol.Cells*, **2011**, *95*, 1421–1436. b) E.Osei-Agyemang, G. Balasubramanian, *Acs. App. Energy Mater*. **2020**, 1, 1139-1144. c) E.Osei-Agyemang, C. E. Adu, G. Balasubramanian, *Adv. Theo. Simu*. **2019**, *2*, 1900060.

[27] Q. Guo, H. W. Hillhouse, R. Agrawal, *J. Am. Chem. Soc.*, **2011**, *131*, 11672–11673.

[28] C. Steinhagen, M. G. Panthani, V. Akhavan, B. Goodfellow, B. Koo, B. A. Korgel,*J.Am. Chem. Soc.*, **2011**, *131*, 12554–12555.

[29] a)M. G.Panthani, V. Akhavan, B. Goodfellow, J. P. Schmidtke, L. Dunn,A. Dodabalapur, P.F. Barbara, B.A. Korgel, *J. Am. Chem. Soc*., **2008**, *130*, 16770–16777; b) P. Jackson, D. Hariskos, E. Lotter, S. Paetel, R. Wuerz, R. Menner, W. Wischmann, M. Powalla, *Photovolt.: Res. Appl.*, **2011**, *19*, 894–897; c) J. Y. Kim, J. Yang, J. H. Yu, W. Baek,C.-Ho Lee, H. J. Son, T. Hyeon, M. J.Ko,*ACS Nano*,**2015**,*9(11)*,11286–11295.

[30] K. O. Klepp, D. Gurtner, *J. Alloys and Compd.*, **1996**, *243*, 19-22.

[31] P. M. Keane, J. A. Ibers, *J. Solid State Chem.*, **1991**, *93*, 291-297.

[32] E. M. Chen, L. Williams, A. Olvera, C. Zhang, M. Zhang, G. Shi, J. T. Heron, L. Qi, L. J. Guo, E. Kioupakis, P. F. P. Poudeu, *Chem. Sci*., **2018**, *9*, 5405-5414.

[33] L. Pauling, R. Hultgren, *Z. Kristallogr.*, **1932**, *84*, 204.

[34] K.O. Klepp, D. Gurtner, *Z. Krystallogr.*, **2000**,*215*, 4.

[35] G. E. Delgado,A. J. Mora, S. Dur´an, M. Mu˜noz, P. G. Gallardo, *J. Alloys and Compd.*, **2007**, *439*, 346–349.

[36]Y. J. Lu, J. A. Ibers,*Journal of Solid State Chemistry* ,**1993**, *107*, 58-62.

[37] G. E. Delgado, A. J. Mora, P. G. Gallardo, S. Durán, M. Muñoz, M. Quintero, *Chalcogenide Letters.* **2009**, *69*, 335 – 338.

[38] A. B. Kehoe, D. O. Scanlon and G. W. Watson, *J.Mater. Chem. C.***2015**, *3*, 12236-12244.

[39] L. Palatinus, G. Chapuis, *Journal of Applied Crystallography*, **2007**, *40*, 786-790.

[40] V. Petříček, M. Dušek, L. Palatinus, The crystallographic computing system, Institute of Physics, *Academy of Sciences of the Czech Republic,* **2006**, 162, 53.

[41] P. Hohenberg, W. Kohn, *Phys.Rev.,* **1964**, *136*, 864−871.

[42] W. Kohn, L. J. Sham, *Phys. Rev.,* **1965**, *140*, 1133−1138.

[43] G. Kresse, J. Hafner, *Phys.Rev.B.*, **1994**, *49*, 14251−14269.

[44] J. P. Perdew, K. Burke, M. Ernzerhof, *Phys.Rev.Lett.***1996**,*77*,3865−3868.

[45] A.Togoand, I. Tanaka, *Scr.Mater.*, **2015**,*108*,1-5.

[46] (a)A. Bhattacharya, *Journal of Materials Chemistry C.* **2019**,*7*, 13986-13992. (b) A. Bhattacharya, *Journal of Physics: Condensed Matter*, **2020**, *32*, 175502.

[47] (a) X. Chen, M. Onoda, H. Wada, A. Sato, H. Herbst-Irmer, *Journal of Solid State Chemistry,* **1999**, *145*, 204 -211. (b) A. Choudhury *et al*. New insights into the structure, chemistry, and properties of Cu_4SnS_4. *Journal of Solid State Chemistry*, **2017**, 253, 192–201.

[48] M. Patel, A. Chavda,I. Mukhopadhyay, J. Kimband, A. Ray, *Nanoscale*, **2016**, *8*, 2293–2303.

[49] J. Tauc, R. Grigorovici and A. Vancu, *Physica Status Solidi*, **1966**, *15*, 627-637.

[50] M. K. Jana, K. Pal, U. V. Waghmare, K. Biswas, *Angew. Chem. Int. Ed.,* **2016**, *55*, 7792−7796.

[51] H. Lin *et al*. *Angew. Chem. Int. Ed.,* **2016**, *55*, 11431−11436.

10.1002/anie.202014222

Keywords: X-ray diffraction, atomic disorder, ultra-low thermal conductivity, phonon dispersion, electronic band structure.

Table of Contents:

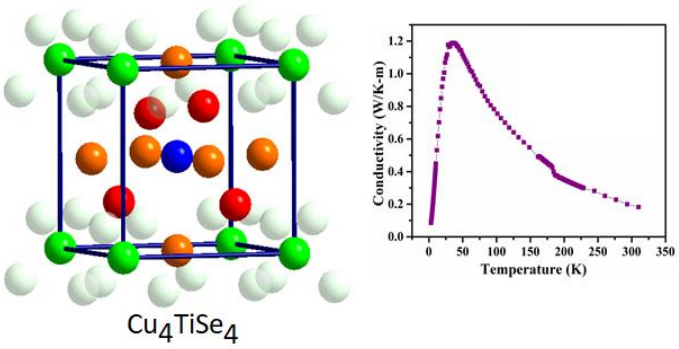

Cu_4TiSe_4

Cu_4TiSe_4 is a unique example of a non-toxic and low-cost material that exhibits lattice ultra-low thermal conductivity of 0.19 W $m^{-1}K^{-1}$ at room temperature. The main contribution to the unusually low thermal conductivity is connected with the atomic lattice and its dynamics.